JOURNAL OF VISUAL COMMUNICATION AND IMAGE REPRESENTATION
Vol. 4, No. 3, September, pp. 242–253, 1993

Optimal PR-QMF Design for Subband Image Coding[1]

H. CAGLAR,[2] Y. LIU, AND A. N. AKANSU

Department of Electrical and Computer Engineering, Center for Communications and Signal Processing Research, New Jersey Institute of Technology, University Heights, Newark, New Jersey, 07102

Received October 2, 1991; accepted January 27, 1993

A multivariable optimization problem is set to design 2-band PR-QMFs. The energy compaction, aliasing energy, unit step response, zero-mean high-pass filter, uncorrelated subband signals, constrained nonlinearity of the phase-response, and the given input statistics are simultaneously considered in the proposed optimal filter design technique. A set of optimal PR-QMF solutions and the optimization criteria along with their objective performance is given for comparison. This PR-QMF design approach leads to an input driven adaptive subband filter bank structure. It is shown that the optimal filters objectively outperform the well-known fixed PR-QMFs in the literature. The proposed PR-QMF design technique provides the mathematical tools for subjective performance improvements in subband image and video coding applications. © 1993 Academic Press, Inc.

I. INTRODUCTION

Two-band Perfect Reconstruction Quadrature Mirror Filters (PR-QMF) have become popular multiresolution signal decomposition tools, particularly for signal coding applications [1–4]. Their modular nature leads to the hierarchical subband trees which have been widely used in the literature. Additionally, it is shown that the 2-band PR-QMFs are the crucial components of the orthonormal wavelet basis design procedures [5, 6].

This paper deals with the optimal 2-band PR-QMF design problem. The approach taken here considers a set of design variables which are of great practical interest in image coding. Some of these variables have been considered earlier in the filter design field, but this study uses them all simultaneously to obtain the optimal solutions.

Section II introduces the variables of optimization problem and their practical significance in image coding. It also discusses their mathematical definitions and lays the ground for the objective function of the optimization. Sections III and IV look into two different sets of optimal PR-QMF design. Section V presents the optimal PR-QMF solutions for different scenarios considered and their comparative performance. Section VI discusses the possible extensions of this research and concludes the paper.

II. VARIABLES OF OPTIMIZATION AND THEIR SIGNIFICANCE IN IMAGE PROCESSING

The proposed optimal PR-QMF design technique considers several parameters of practical significance in the filter design. These parameters, namely, the energy compaction, aliasing energy, unit step response, zero-mean high-pass filter, uncorrelated subband signals, constrained nonlinear phase response, and input statistics are combined to define the objective function of the optimization problem. Some of these features have been well known in the filter design field and used by several researchers in the literature. For example, Johnston has considered the aliasing minimization in his QMF design procedure [7]. Additionally, it is a classical approach for filter design to minimize the stop band energy. This study intuitively benefited from the earlier work in the field but also has significant improvements in the solution of PR-QMF problems particularly for image coding applications. We included the following variables in the design of optimal PR-QMFs:

(*a*) *Orthonormal PR Requirement.* This set of requirements is included in the design to obtain the unitary perfect reconstruction condition which is of interest here. The orthonormal PR condition is important particularly in signal coding applications.

The high-pass filter is assumed to be the mirror of the half-bandwidth low-pass filter $\{h(n)\}$ of length $2N$ which is also expressed in the vector form $\mathbf{h}$. Hence the unitary condition of the filter can easily be written in vector product form as

$$\mathbf{h}^T\mathbf{h} = 1. \tag{1}$$

The perfect reconstruction condition of orthonormal 2-band PR-QMF is easily shown as [1–5]

$$\sum_n h(n)h(n + 2k) = \delta(k). \tag{2}$$

[1] This paper was presented in part at SPIE Visual Communication and Image Processing, Boston, Nov. 1991.

[2] Present address: TUBITAK Research Center, Gebze, Turkey.

1047-3203/93 $5.00

Equations (1) and (2) can be combined in the matrix form

$$\mathbf{h}^T C_i \mathbf{h} = 0 \quad i = 1, 2, \ldots, N-1, \tag{3}$$

where C_i are the proper *filter coefficient shuffling matrices* as

$$C_1 = \begin{bmatrix} 0 & 0 & 1 & 0 & \ldots & 0 \\ 0 & 0 & 0 & 1 & \ldots & 0 \\ 1 & 0 & 0 & 0 & \ldots & 0 \\ \vdots & \vdots & & & & \vdots \\ 0 & 0 & 1 & 0 & \ldots & 1 \\ 0 & 0 & 0 & 1 & \ldots & 0 \\ 0 & 0 & 0 & 0 & \ldots & 0 \end{bmatrix}, \ldots,$$

$$C_{N-1} = \begin{bmatrix} 0 & 0 & 0 & \ldots & 1 & 0 \\ 0 & 0 & 0 & \ldots & 0 & 1 \\ 0 & 0 & 0 & \ldots & 0 & 0 \\ 0 & 0 & 0 & \ldots & 0 & 0 \\ \vdots & \vdots & & & \vdots & \vdots \\ 1 & 0 & 0 & \ldots & 0 & 0 \\ 0 & 1 & 0 & \ldots & 0 & 0 \end{bmatrix}. \tag{4}$$

Equation (3) is satisfied as a part of the optimal filter solutions introduced later.

(*b*) *Energy Compaction.* This is a desired feature for any orthonormal signal decomposition technique. Energy compaction measure is derived with the help of the rate-distortion theory. The significance and the derivation of this measure can be found in Ref. [8]. This performance measure has been widely used in the literature for the comparison of different signal decomposition techniques [4, 8]. Reference [13] deals with the optimal design of PR-QMFs based on this measure only.

The output energy of the low pass filter $h(n)$ for the given covariance matrix R_{xx} of a zero-mean input can be expressed as

$$\sigma_L^2 = \mathbf{h}^T R_{xx} \mathbf{h}. \tag{5}$$

We are now looking for the optimal PR-QMF solution which maximizes Eq. (5). It is clear that this will be sufficient condition to maximize the energy compaction measure, gain of transform coding over PCM(G_{TC}), which is given for the 2-band case as

$$G_{TC} = \frac{\sigma_x^2}{(\sigma_L^2 \sigma_H^2)^{1/2}} = \frac{\sigma_x^2}{\sigma_L \sigma_H}. \tag{6}$$

The input signal variance is related to the band variances, σ_L^2 and σ_H^2, in the unitary case as

$$\sigma_x^2 = \frac{1}{2}(\sigma_L^2 + \sigma_H^2).$$

(*c*) *Aliasing Energy.* All of the orthonormal signal decomposition techniques satisfy the conditions of alias cancellation for perfect reconstruction. In practice, since all the bands are not used for the synthesis or the different levels of quantization noise in subbands, the noncancelled aliasing energy components exist in the reconstructed signal. Its significance has been noticed in image processing applications. It is observed that the aliasing causes annoying patterns in encoded images at low bit-rates.

The aliasing energy component for the low-pass filter output in 2-band PR-QMF bank can be written for the given input spectral density function $S_{xx}(e^{j\omega})$ [9]

$$\sigma_A^2 = \frac{1}{2\pi} \int_{-\pi}^{\pi} |H(e^{-j\omega})|^2 \, S_{xx}(e^{j(\omega+\pi)}) | \, H(e^{j(\omega+\pi)})|^2 d\omega. \tag{7}$$

The time-domain counterpart of this relation is easily found as

$$\sigma_A^2 = \sum_k [\rho(n) * (-1)^n \rho(n)] \, R_{xx}(k), \tag{8}$$

where $\rho(n)$ is the autocorrelation sequence of the filter $h(n)$ and defined as

$$\rho(n) = h(n) * h(-n).$$

$R_{xx}(k)$ is the autocorrelation sequence of the input. The optimal solution searched should minimize the aliasing energy component of the low-pass filter output, Eq. (8), in 2-band PR-QMF case.

Differently from the earlier design procedures in the literature, the aliasing energy is related to the spectral density of the input. The former designs have emphasized on the flat frequency response implying flat input spectrum.

(*d*) *Unit Step Response.* The representation of edges in images is a crucial problem. The edge structures are localized in time therefore they should be represented by the time-localized basis functions. Otherwise the ringing artifacts occur in encoded images. An edge can be considered as a step. Therefore the step responses of the filters in the filter banks should be considered during the design procedure [10].

It is a well-known phenomenon called the uncertainty principle which states that a signal can not be localized perfectly in one domain without the worst concentration

in the other [11]. The human visual system is able to resolve the time–frequency plane therefore a joint time-frequency localization should be considered in a practically meritful filter bank design [12]. The trade-off between the time and frequency resolutions is reflected in the aliasing and step response characteristics of the filters.

The unit step response of the filter $h(n)$ can be written as

$$a(n) = h(n) * u(n),$$

where $u(n)$ is the unit step sequence. The difference energy between the unit step response $a(n)$ of the filter and the unit step sequence $u(n)$ is expressed as

$$E_s = \sum_{k=0}^{2N-1} \left[\sum_{n=0}^{k} h(n) - 1 \right]^2. \tag{9}$$

E_s is minimized for the optimal solution. The optimization variable E_s does not consider the symmetry of the unit step response around the step point. This point is addressed later since it is directly related to the linear phase condition of the filter.

(e) Zero Mean High-Pass Filter. Most of the practical signal sources have their significant energy located around the DC frequency. Therefore useful signal decomposition techniques should be able to represent the DC frequency component within only one basis function. Following this argument one should constrain the high-pass QMF function to have zero mean as

$$\sum_n (-1)^n h(n) = 0. \tag{10}$$

This requirement implies that there should be at least one zero of the low pass filter $h(n)$ at $\omega = \pi$. This condition implies a degree of regularity in wavelet transform context [5].

(f) Uncorrelated Subband Signals. It is a well-known fact in signal coding field that any good signal representation technique should be able to provide uncorrelated transform coefficients or subband signals. The Karhunen–Loeve Transform (KLT) [8] is the unique example of this characteristic in the block transforms. It is noteworthy that the uncorrelatedness and the maximum energy compaction requirements merge in the KLT solutions of block transforms. But this is not true in the filter banks. The filter bank solutions with this desired feature are sought.

The cross-correlation of the two subband signals for the given input is defined as

$$E\{y_L(m)y_H(m)\} = R_{LH}(0) = \sum_n \left[\sum_l h(l)(-1)^l h(n-l) \right] R_{xx}(n) \quad \text{for all } m. \tag{11}$$

In general, there are more than one filter solutions which satisfy the condition $R_{LH}(0) = 0$. Obviously the one which maximizes the objective function is the meaningful solution.

(g) Constrained Nonlinearity in Phase Response. Since there cannot be any linear-phase orthonormal 2 equal band PR-QMF solution, the linearity condition on the phase responses of the filter functions is relaxed. Linear phase and PR are two conflicting conditions in orthonormal 2-band QMF design. But, it is also known that the severe phase nonlinearities create undesired degradations in image and video applications. Therefore, a measure which indicates the level of nonlinearity in the phase response is included as a parameter in the optimal design. Nonlinearity measure of the phase response is related to the nonsymmetry of the unit sample response and defined as

$$E_p = \sum_n (h(n) - h(2N-1-n))^2. \tag{12}$$

E_p is minimized in optimal filter solutions.

(h) Given Input Statistics. The characteristics of the input spectral density function are very important for the variables of optimal design. The whole optimization procedure is related to the given input statistics. This will also lead to the input driven filter bank solutions which may be useful in some of the applications with the nonstationary sources. This study assumes as autoregressive, order 1, $AR(1)$ source model with the correlation coefficient $\rho = 0.95$ which is a crude approximation to the real world still frame images. The correlation sequence of this source is expressed as

$$R_{xx}(m) = \rho^{|m|} \quad m = 0, \pm 1, \pm 2, \ldots. \tag{13}$$

From Eq. (13), the corresponding Toeplitz covariance matrix R_{xx} is easily obtained.

These variables of the optimization are included in the objective function and the set of constraints considered simultaneously. There are many filter bank solutions available based on different objective functions and parameter sets. We present the examples of objective functions to be optimized in the following two sections.

III. OPTIMAL PR-QMF DESIGN BASED ON ENERGY COMPACTION

This optimization problem consists of the PR and energy compaction conditions as defined in Eqs. (3) and (5), for an $AR(1)$ source with $\rho = 0.95$.

We now set the objective function J which is to be maximized as

$$\max\{J\} = \mathbf{h}^T R_{xx}\mathbf{h} + \lambda_0[1 - \mathbf{h}^T\mathbf{h}] + \lambda_1[\mathbf{h}^T C_1\mathbf{h}] + \cdots + \lambda_i[\mathbf{h}^T C_i\mathbf{h}]. \quad (14)$$

Hence,

$$\frac{\partial J}{\partial \mathbf{h}} = 0,$$

therefore,

$$R_{xx}\mathbf{h} + \lambda_1 C_1\mathbf{h} + \cdots + \lambda_i C_i\mathbf{h} = \lambda_0\mathbf{h}. \quad (15)$$

If the terms in the left side of the equation are combined as

$$R\mathbf{h} = \lambda_0\mathbf{h}, \quad (16)$$

where

$$R = R_{xx} + \lambda_1 C_1 + \cdots + \lambda_i C_i.$$

Equation (16) looks like a classical eigenvalue problem but here the matrix R has unknown parameters in it. The vector $\mathbf{h}$ which satisfies Eq. (16) is the optimal low-pass PR-QMF. It is clear that this objective function implicitly considers only the frequency behavior of the filter.

IV. OPTIMAL PR-QMF DESIGN BASED ON EXTENDED SET OF VARIABLES

The aliasing energy, unit step response, constrained nonlinear phase characteristics, zero-mean high-pass filter, uncorrelated subband requirements additional to Eq. (14) are included in the objective function. The optimization problem is now set as

$$\max\{J\} = \mathbf{h}^T R_{xx}\mathbf{h} - \alpha \sum_k [\rho(n) * (-1)^n \rho(n)]\, R_{xx}(k) - \beta \sum_{k=0}^{2N-1} \left[\sum_{n=0}^{k} h(n) - 1\right]^2 - \gamma \sum_n [h(n) - h(2N - 1 - n)]^2, \quad (17)$$

with the set of unitary, PR, zero-mean high-pass filter, and uncorrelated subband signals constraints as

$$\sum_n h(n)h(n + 2k) = \delta(k)$$
$$\sum_n (-1)^n h(n) = 0 \quad (18)$$
$$R_{LH}(0) = 0.$$

This is a very general optimization problem that jointly addressing the time and frequency domain behavior of the filter. There are a set of parameters in the objective function which should be fine tuned for the application considered. Therefore, the proposed optimal filter design approach should be supported with the experimental studies. The significance of the optimization variables in the objective function should be quantified for the human visual system. The following section presents examples of the optimal filters and their problem definitions.

V. OPTIMAL PR-QMF SOLUTIONS AND THEIR PERFORMANCE

Since there is a set of parameters in the optimization problems defined earlier the possible filter solutions are many. Therefore, we studied the interrelations of the optimization variables. In this framework, we first attempt to relate the energy compaction and aliasing energy of the 2-band PR-QMF as defined in Eqs. (6) and (8), respectively. Figure 1a displays this relation for 8-tap filter solutions and $AR(1)$ source with $\rho = 0.95$. As seen from the figure, this relation is linear-like and the energy compaction increases as the aliasing energy decreases. This trend is easily justified. The optimal PR-QMF solutions obtained are also consistent with this figure. Figure 1b displays the relation of energy compaction and interband correlations again for the same source model. Although these two variables merge in the unique optimal solutions of block transforms, *KLT*, it is not true for the filter banks. In other words, there are more than one possible solutions. One should pick the solution which maximizes the objective function. Therefore the relations of uncorrelated interband and the energy compaction in filter banks are not as clear as in the block transforms. This point deserves further studies.

Figure 1c displays the relations of 2-band energy compaction and the level of nonlinearities in the phase responses of 8-tap filters.

Figure 1d provides the relations of 2-band energy compaction and the imperfectness of filter unit step responses. This plot indicates that whenever the unit step response gets closer to the unit step function the energy compaction decreases. This relation clearly questions the practical merit of the energy compaction measure. Energy compaction measure implies the frequency localization of the filter for the source considered. On the other hand, the step response is related to the time localization. The practical trade-offs for the time and frequency localizations of filters deserve further studies.

Table 1 displays the coefficients of 4-, 6-, 8-, 12-, and 16-tap optimal PR-QMFs based on energy compaction criterion with zero-mean high-pass constraint. Similarly, Table 2, gives the optimal PR-QMF coefficients based on minimized aliasing energy with zero-mean high-pass. Table 3 has the optimal PR-QMFs similar to Table 1, but additionally providing uncorrelated subbands or $R_{LH}(0) =$

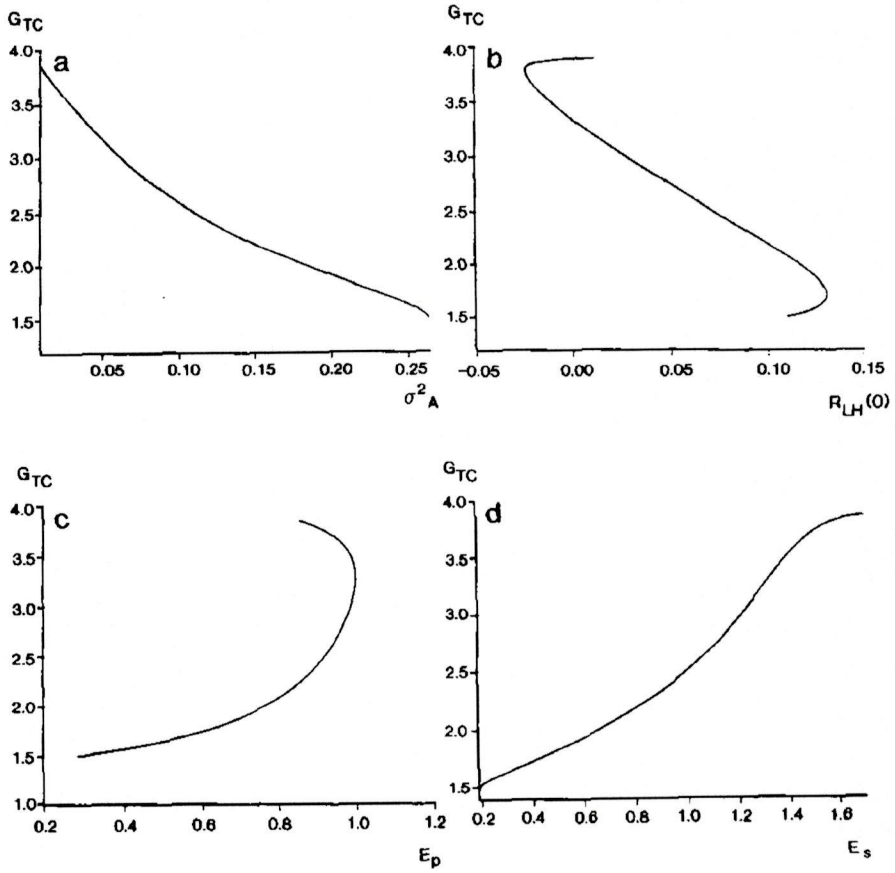

FIG. 1. The relations of (a) G_{TC} versus σ^2_A, (b) G_{TC} versus $R_{LH}(0)$, (c) G_{TC} versus E_p, and (d) G_{TC} versus E_s of 8-tap, 2-band PR-QMFs for $AR(1)$, $\rho = 0.95$ source.

0 for $AR(1)$ source with $\rho = 0.95$. Table 4 also adds this constraint to the conditions of Table 2.

Table 5 gives the optimal filters based on extended objective function of Eq. (17) with the weight variations only in the phase response. Similarly, Table 6 provides the optimal filter coefficients with the weight variations in the unit step response of Eq. (17). These solutions were obtained by using the IMSL FORTRAN library (routine NCONF). The package solves a general nonlinearly constrained minimization problem using the successive quadratic programming algorithm and a finite difference gradient.

All of the solutions displayed in the tables assume $AR(1)$ source of $\rho = 0.95$. The table also includes the performance of the filters for comparison.

VI. DISCUSSION AND CONCLUSIONS

We have developed a framework to design statistically optimized 2-band PR-QMFs suitable for subband image coding. This procedure considers the effects of the uncertainty principle in the time–frequency signal analysis. This is succeeded implicitly by considering the effects of aliasing energy and the unit step response of the designed PR-QMFs for the given input statistics.

The proposed approach considers several practical parameters of image coding in the optimization problem. There are quite a few possible filter solutions with this approach. Therefore, the parameters of the optimization should be tuned to the human visual system with the experimental studies for subjectively optimal PR-QMF solutions.

The variables of optimization considered in this paper shape the time–frequency cell of designed filter or basis function. Some of those variables, e.g., energy compaction, aliasing energy, emphasize the frequency domain localization of the filter while some others, e.g., unit step response, phase response, emphasize the time domain localization. The uncertainty principle states that a function can not localize simultaneously in both domains. Therefore, there is a trade-off to be monitored in the design for the application at hand [15, 16].

Table 7 displays the objective performance of Binomial QMF-wavelet filters [6, 5], Smith–Barnwell CQF [1] and

TABLE 1
A Set of Optimal PR-QMF Filter Coefficients and Their Performance

n	$h(n)$	$h(n)$	$h(n)$	$h(n)$	$h(n)$
0	0.201087342	0.244206457	0.317976535	0.385659639	0.482962940
1	0.600007520	0.664513457	0.748898833	0.796281177	0.836516297
2	0.665259025	0.629717438	0.534939876	0.428145720	0.224143841
3	0.198773686	0.089423027	−0.058836349	−0.140851286	−0.129409515
4	−0.233790239	−0.251577216	−0.205817322	−0.106698578	
5	−0.153612998	−0.072467574	0.042523091	0.051676890	
6	0.118834741	0.134086583	0.060007692		
7	0.101350938	0.031916868	−0.025478793		
8	−0.074934374	−0.076499461			
9	−0.061434875	0.003706982			
10	0.053218300	0.027172980			
11	0.029837627	−0.009985979			
12	−0.037981695				
13	−0.002649357				
14	0.015413680				
15	−0.005165762				
G_{TC}	3.9220	3.9038	3.8548	3.7961	3.6426
σ_A^2	0.0056	0.0075	0.0115	0.0153	0.0239
R_{LH} (0)	0.0040	−0.1601	−0.0140	−0.0160	−0.0422
Mean	0.0000	0.0000	0.0000	0.0000	0.0000
E_p	1.0622	1.0320	0.8566	1.2506	0.7500
E_s	3.3613	2.5730	1.7493	1.3059	0.8365

Note. The optimality is based on energy compaction with zero mean high-pass filter.

TABLE 2
A Set of Optimal PR-QMF Filter Coefficients and Their Performance

n	$h(n)$	$h(n)$	$h(n)$	$h(n)$	$h(n)$
0	0.239674169	0.276769143	0.339291195	0.398655794	0.482962940
1	0.641863878	0.689345705	0.753812779	0.792728512	0.836516297
2	0.628941341	0.592445147	0.510688095	0.420459801	0.224143841
3	0.136154317	0.054082233	−0.062731472	−0.141949922	−0.129409515
4	−0.241530316	−0.247471430	−0.210405609	−0.112008814	
5	−0.123175317	−0.059746881	0.046422128	0.056328191	
6	0.128959373	0.138373438	0.067533100		
7	0.088433853	0.031525301	−0.030396654		
8	−0.083586814	−0.088498729			
9	−0.058991180	0.006149179			
10	0.061697343	0.035489212			
11	0.033431236	−0.014248756			
12	−0.050042508				
13	−0.002023897				
14	0.022994193				
15	−0.008586110				
G_{TC}	3.9189	3.9002	3.8513	3.7935	3.6426
σ_A^2	0.0054	0.0073	0.0113	0.0152	0.02397
R_{LH} (0)	0.0001	−0.1849	−0.0170	−0.0138	−0.0422
Mean	0.0000	0.0000	0.0000	0.0000	0.0000
E_p	1.0521	0.9933	0.8450	1.2520	0.7500
E_s	3.2836	2.5202	1.7232	1.2930	0.8365

Note. The optimality is based on minimized aliasing energy with zero mean high-pass filter.

TABLE 3
A Set of Optimal PR-QMF Filter Coefficients and Their Performance

n	$h(n)$	$h(n)$	$h(n)$	$h(n)$	$h(n)$
0	0.224159871	−0.106117265	0.240118698	0.312656005	0.000000000
1	0.629151335	−0.041624773	0.688564034	0.754045521	0.707106781
2	0.642510825	0.444275957	0.638286732	0.543768338	0.707106781
3	0.158071546	0.761031030	0.017567002	−0.108851490	0.000000000
4	−0.240893371	0.427762258	−0.235301591	−0.149317562	
5	−0.133127916	−0.066013158	0.023295098	0.061912751	
6	0.128098122	−0.107784207	0.064002943		
7	0.090074845	0.085537312	−0.022319352		
8	−0.081998711	0.051558425			
9	−0.055306473	−0.038422405			
10	0.058081519	−0.002588387			
11	0.026452620	0.006598776			
12	−0.040400680				
13	−0.001956582				
14	0.017549205				
15	−0.006252594				
G_{TC}	3.9207	3.8935	3.8408	3.7661	3.2025
σ_A^2	0.0055	0.0083	0.0126	0.0167	0.0487
R_{LH} (0)	0.0000	0.0000	0.0000	0.0000	0.0000
Mean	0.0000	0.0000	0.0000	0.0000	0.0000
E_p	1.0531	0.8694	0.9011	1.3048	0.0000
E_s	3.3117	4.4123	1.8685	1.3968	1.4289

Note. The optimality is based on energy compaction with zero mean high-pass and uncorrelated subband signals.

TABLE 4
A Set of Optimal PR-QMF Filter Coefficients and Their Performance

n	$h(n)$	$h(n)$	$h(n)$	$h(n)$	$h(n)$
0	0.240173769	−0.121396419	0.249509936	0.348319026	0.000000000
1	0.642454295	−0.035246082	0.688584306	0.758774508	0.707106781
2	0.628348271	0.467924401	0.632097530	0.510327483	0.707106781
3	0.135389521	0.751312762	0.015778256	−0.121232755	0.000000000
4	−0.241606760	0.412397276	−0.240993887	−0.151539728	
5	−0.122763195	−0.062892458	0.026838168	0.069565029	
6	0.129125126	−0.109012591	0.066493202		
7	0.088184458	0.093200632	−0.024093948		
8	−0.083719165	0.059816603			
9	−0.058849491	−0.048300585			
10	0.061801498	−0.002622488			
11	0.033339516	0.009032511			
12	−0.050088120				
13	−0.002023074				
14	0.023072163				
15	−0.008625249				
G_{TC}	3.9188	3.8897	3.8399	3.7611	3.2025
σ_A^2	0.0054	0.0083	0.0126	0.0165	0.0487
R_{LH} (0)	0.0000	0.0000	0.0000	0.0000	0.0000
Mean	0.0000	0.0000	0.0000	0.0000	0.0000
E_p	1.0518	0.8667	0.8941	1.3052	0.0000
E_s	3.2826	4.4280	1.8564	1.3539	1.4289

Note. The optimality is based on minimized aliasing energy with zero mean high-pass and uncorrelated subband signals.

TABLE 5
Optimal PR-QMF Filter Solutions and Their Performance

	$\alpha = 0.5, \beta = 0.01, \gamma = 0.01$				
n	$h(n)$	$h(n)$	$h(n)$	$h(n)$	$h(n)$
0	0.349996497	0.360838504	0.377995233	0.442766931	0.466675669
1	0.731063819	0.744306049	0.768367237	0.805049213	0.840588657
2	0.505852096	0.490757098	0.462086554	0.352529377	0.240431112
3	−0.010803415	−0.036047928	−0.86013220	−0.146445561	−0.133481875
4	−0.229358399	−0.222383198	−0.194919256	−0.088189527	
5	−0.029975411	−0.005408341	0.055225994	0.048503129	
6	0.134362313	0.128127832	0.061944250		
7	0.026991307	0.000007678	−0.030473229		
8	−0.089102151	−0.079675397			
9	−0.017502278	0.018522733			
10	0.062860841	0.029441941			
11	0.006564367	−0.014273411			
12	−0.045242724				
13	0.009260600				
14	0.017738308				
15	−0.008492207				
G_{TC}	3.8950	3.8809	3.8432	3.7829	3.6407
σ_A^2	0.0065	0.0080	0.0115	0.0158	0.0240
R_{LH} (0)	−0.0084	−0.2052	−0.0196	−0.01970	−0.0437
Mean	0.0000	0.0000	0.0000	0.0000	0.0000
E_p	0.9859	0.9439	0.8432	1.2022	0.7303
E_s	3.1015	2.395	1.6745	1.2436	0.8503

Note. The optimality is based on Eq. (17) and only the weight of the phase response variable is changed.

	$\alpha = 0.5, \beta = 0.01, \gamma = 0.1$				
n	$h(n)$	$h(n)$	$h(n)$	$h(n)$	$h(n)$
0	0.570782868	0.569472913	0.568917465	0.592766220	0.587090288
1	0.773403148	0.775299669	0.779977112	0.780949238	0.795662560
2	0.207871420	0.208282686	0.205671595	0.156911420	0.120016493
3	−0.101404580	−0.103659132	−0.112813827	−0.106155142	−0.088555779
4	−0.101233393	−0.101645713	−0.092613815	−0.042570859	
5	0.040562313	0.044417637	0.058274508	0.032312685	
6	0.064121473	0.064537457	0.025131536		
7	−0.022088292	−0.029119506	−0.018331012		
8	−0.048700901	−0.045720022			
9	0.017118797	0.029114167			
10	0.039132815	0.012179460			
11	−0.015973034	−0.008946054			
12	−0.032702905				
13	0.021271073				
14	0.007835404				
15	−0.005782643				
G_{TC}	3.6246	3.6274	3.6272	3.5769	3.5554
σ_A^2	0.0216	0.0217	0.0224	0.0262	0.0283
R_{LH} (0)	−0.0083	−0.2195	−0.0171	−0.0149	−0.0274
Mean	0.0000	0.0000	0.0000	0.0000	0.0000
E_p	0.9682	0.9580	0.9367	1.0614	0.9129
E_s	2.8281	2.1435	1.4567	1.0846	0.7413

TABLE 5—*Continued*

	$\alpha = 0.5, \beta = 0.01, \gamma = 0.5$				
n	$h(n)$	$h(n)$	$h(n)$	$h(n)$	$h(n)$
0	0.436459489	0.468918374	0.893161751	0.883792413	0.851141192
1	0.770165754	0.754465714	0.196575502	0.226143909	0.304498519
2	−0.210563240	−0.223237677	−0.055961409	−0.080641139	−0.144034410
3	0.076322596	−0.091820497	0.061848233	0.105611642	0.402608262
4	−0.015358635	−0.010004074	−0.047017781	−0.096044493	
5	−0.001475061	0.003575508	0.071219382	0.375351230	
6	0.007791289	0.042639010	−0.083075780		
7	−0.006978594	0.007741037	−0.377463664		
8	0.013431262	0.116547022			
9	−0.002821529	0.043571171			
10	0.032517339	0.312244125			
11	0.011528011	−0.194067146			
12	0.105043470				
13	0.051791696				
14	0.337785806				
15	−0.191426092				
G_{TC}	1.3138	1.5253	1.5600	1.7714	2.1612
σ_A^2	0.3707	0.2724	0.2590	0.1979	0.1280
R_{LH} (0)	−0.2241	−0.3795	0.1232	0.0877	0.0478
Mean	0.0000	0.0000	0.0000	0.0000	0.0000
E_p	0.6532	0.7087	0.3721	0.3970	0.4023
E_s	1.0674	1.0822	0.2193	0.2177	0.2180

TABLE 6
Optimal PR-QMF Filter Solutions and Their Performance

	$\alpha = 0.5, \beta = 0.01, \gamma = 0.00$				
n	$h(n)$	$h(n)$	$h(n)$	$h(n)$	$h(n)$
0	−0.072118727	−0.140400385	0.338751710	0.414924083	0.450726782
1	0.032229491	−0.150338392	0.753050835	0.802108334	0.844019834
2	0.472159777	0.297817459	0.512178433	0.389177069	0.256379999
3	0.728661982	0.716925775	−0.062729040	−0.145175948	−0.136913053
4	0.412106727	0.562813589	−0.210590019	−0.966994371	
5	−0.089723281	0.074485419	0.046819239	0.050174395	
6	−0.180228443	−0.101597229	0.066766657		
7	0.058425583	0.069475983	−0.030034253		
8	0.122112963	0.120498364			
9	−0.041446572	−0.033350030			
10	−0.076759955	−0.032025017			
11	0.044183696	0.029908027			
12	0.028424519				
13	−0.028379044				
14	0.001409920				
15	0.003154926				
G_{TC}	3.9135	3.8988	3.8516	3.7928	3.6357
σ_A^2	0.0060	0.0073	0.0113	0.0154	0.0243
R_{LH} (0)	−0.0049	−0.0412	−0.0165	−0.0183	−0.0450
Mean	0.0000	0.0000	0.0000	0.0000	0.0000
E_p	0.9063	0.7827	0.8454	1.2269	0.6906
E_s	4.7944	5.1120	1.7241	1.2735	0.8638

Note. The optimality is based on Eq. (17) and only the weight of the step response variable is changed.

TABLE 6—*Continued*

$\alpha = 0.5, \beta = 0.1, \gamma = 0.00$

n	$h(n)$	$h(n)$	$h(n)$	$h(n)$	$h(n)$
0	0.051858566	−0.055559533	0.377668686	0.531436244	0.000000000
1	0.380482562	0.289422202	0.749142516	0.825711921	0.707106760
2	0.712802256	0.758607778	0.474281619	0.155148903	0.707106760
3	0.420775226	0.396381623	−0.055253895	−0.105397216	0.000000000
4	−0.081862324	−0.027600992	−0.234063349	0.020521635	
5	−0.052470327	0.175485587	0.058196964	−0.013207924	
6	0.067027296	0.059980247	0.089219826		
7	−0.0159621296	−0.326344975	−0.044978804		
8	−0.071890824	0.033259598			
9	0.240675222	0.183983737			
10	0.024453215	−0.061580317			
11	0.0220059481	−0.011821393			
12	0.059265979				
13	0.085890240				
14	−0.054547383				
15	0.007434635				
G_{TC}	3.5895	3.3675	3.8112	3.5753	3.2025
σ_A^2	0.0174	0.0255	0.0124	0.0275	0.0487
R_{LH} (0)	0.0120	−0.0422	−0.0199	−0.0414	0.0000
Mean	0.0000	0.0000	0.0000	0.0000	0.0000
E_p	0.7792	0.6897	0.8192	1.0128	0.0000
E_s	3.7582	3.3832	1.6791	1.1293	1.4289

$\alpha = 0.5, \beta = 0.5, \gamma = 0.00$

n	$h(n)$	$h(n)$	$h(n)$	$h(n)$	$h(n)$
0	−0.036394166	0.009777307	0.000000000	0.000000000	0.000000000
1	−0.010653820	0.009950661	0.707106760	0.707106760	0.707106760
2	0.120319736	0.009163096	0.000000000	0.000000000	0.707106760
3	0.018782806	−0.100904704	0.000000000	0.000000000	0.000000000
4	−0.284341438	0.114277633	0.000000000	0.707106760	
5	0.071695457	0.689177732	0.000000000	0.000000000	
6	0.546197426	0.687908298	0.707106760		
7	0.315291373	0.111809215	0.000000000		
8	0.326491983	−0.124581108			
9	0.530216883	0.007451436			
10	0.065344861	0.010561555			
11	−0.314416472	−0.010377558			
12	−0.028986451				
13	0.090980470				
14	−0.001525171				
15	0.005210085				
G_{TC}	3.4726	3.1863	1.5786	1.9429	3.2025
σ_A^2	0.174	0.0140	0.2006	0.1324	0.0487
R_{LH} (0)	−0.0103	−0.0057	0.0000	0.0000	0.0000
Mean	0.0000	0.0000	0.0000	0.0000	0.0000
E_p	0.0062	0.0009	0.0000	0.0000	0.000
E_s	8.4601	6.1696	1.7720	1.6005	1.4289

maxregular wavelet filters [14] for comparison. It is seen that the statistically optimized PR-QMFs introduced in this paper objectively perform better than these well-known PR-QMFs in the literature. The proposed PR-QMF design approach should be incorporated in image, video processing and coding applications to prove its practical merits. The effects of quantization in subband coding are also very important in practice. Recently, Westerink *et al.* [17] attempted to model the quantization noise and combine it with the subband structure. The

TABLE 7
Objective Performance of Binomial QMF-Wavelet Filters [6, 5], Smith–Barnwell CQF [1], and Maxregular Wavelet Filters [14] Based 2-Band Subband Decomposition for $AR(1)$, $\rho = 0.95$, Source

Filter	G_{TC}	σ_A^2	$R_{LH}(0)$	Mean	E_p	E_s
Binomial-QMF (8-tap)	3.8109	0.0147	0.0003	0.0000	0.9085	1.8637
Binomial-QMF (6-tap)	3.7588	0.0177	−0.0233	0.0000	1.2386	1.3550
Binomial-QMF (4-tap)	3.6426	0.0240	−0.0422	0.0000	0.7500	0.8365
Smith–Barnwell (8-tap)	3.8391	0.0127	0.0302	0.0142	0.6008	4.2500
Maxregular (6-tap)	3.7447	0.0185	−0.0103	0.0000	1.2703	1.4446

effects of quantization noise can also be considered in the design of filter banks. This is a topic for future research.

It should also be emphasized that some of the characteristics considered in the proposed PR-QMF design procedure may not be significant in the 2-band case. However, when a hierarchical subband tree structure based on 2-band PR-QMFs is employed all of these characteristics become important [9]. Therefore, they all should be considered simultaneously in the design.

This approach can be extended for M-band (equal or unequal bandwidths) PR filter bank problem. The procedure in that case is computationally complex for the larger values of M.

REFERENCES

1. M. Smith and T. P. Barnwell, Exact reconstruction techniques for tree structure subband coders, *IEEE Trans. ASSP*, 1986, 434–441.
2. M. Vetterli and D. LeGall, Perfect reconstruction FIR filter banks: Some properties and factorizations, *IEEE Trans. ASSP*, July 1989, 1051–1071.
3. P. P. Vaidyanathan, Quadrature mirror filter banks, M-band extensions and perfect reconstruction techniques, *IEEE ASSP Mag* July 1987, 4–20.
4. A. N. Akansu, and Y. Liu, On signal decomposition techniques, *Opt. Eng.* July 1991, 912–920.
5. I. Daubechies, Orthonormal bases of compactly supported wavelets, *Comm. Pure Appl. Math.* **XLI**, 1988, 909–996.
6. A. N. Akansu, R. A. Haddad, and H. Caglar, The binomial QMF-wavelet transform for multiresolution signal decomposition, *IEEE Trans. ASSP*, Jan. 1993, 13–19.
7. J. D. Johnston, A filter family designed for use in quadrature mirror filter banks, *Proc. IEEE ICASSP*, Apr. 1980, 291–295.
8. N. S. Jayant, and P. Noll, *Digital Coding of Waveforms*, Prentice–Hall, Englewood Cliffs, New Jersey, 1984.
9. A. N. Akansu and R. A. Haddad, *Multiresolution Signal Decomposition: Transforms, Subbands, and Wavelets*, Academic Press, San Diego, 1992.
10. T. Kronander, *Some Aspects of Perception Based Image Coding*, Ph.D. Thesis, Lipkoping University, 1989.
11. D. Gabor, Theory of Communications, *Proc. IEE*, 1946, 429–461.
12. T. Caelli, and M. Hubner, Coding images in the frequency domain: filter design and energy processing characteristics of the human visual system, *IEEE Trans. Systems Man Cybernet*, May 1980, 1018–1021.
13. J. Katto and Y. Yasuda, Performance evaluation of subband coding and optimization of its filter coefficients, *Proc. SPIE VCIP*, Nov. 1991, 95–106.
14. I. Daubechies, *Orthonormal Bases of Compactly Supported Wavelets. II. Variations on a Theme*, Technical Memo. no. 11217-891116-17, AT&T Bell Labs, Murray Hill, New Jersey, also private communication.
15. Y. Liu and A. N. Akansu, An evaluation of time–frequency localization in transforms and filter banks, *Proc. IEEE ICASSP*, 1993.
16. R. A. Haddad, A. N. Akansu, and A. Benyassine, Time–frequency localization in transforms, subbands, and wavelets: A critical review, *Opt. Eng.* July 1993.
17. P. H. Westerink, J. Biemond, and D. E. Boekee, Scalar quantization error analysis for image subband coding using QMF's, *IEEE Trans. Signal Process.*, Feb. 1992, 421–428.

HAKAN CAGLAR received the B.S. degree from the Technical University of Istanbul (ITU), Turkey, the M.S. degree from Polytechnic University, and the Ph.D. degree from New Jersey Institute of Technology, all in electrical engineering, in 1984, 1988, and 1991, respectively. He joined the Scientific and Technical Research Center (TUBITAK), Space Sciences Department of Turkey in 1992. His current research interests are digital signal processing, transform techniques for image-video processing and compression, remote sensing, and classification techniques.

YIPENG LIU received her B.S. and M.S. degrees from Beijing Institute of Technology in 1984 and 1987, respectively, both in electrical

engineering. She was a faculty member at Beijing Institute of Technology from 1987 to 1989. She has been with the Department of Electrical and Computer Engineering, New Jersey Institute of Technology, as a Ph.D. student since 1989. Her current research interests are signal decomposition techniques, image processing, and coding.

ALI N. AKANSU received the B.S. degree from the Technical University of Istanbul (ITU), Turkey, in 1980, the M.S. degree from the Polytechnic Institute of New York, Brooklyn, NY, in 1983, and the Ph.D. degree from the Polytechnic University, Brooklyn, NY, in 1987, all in electrical engineering. Since 1987, he has been at the New Jersey Institute of Technology, where he is currently an Associate Professor of Electrical Engineering. He was an Academic Visitor at the IBM T.J. Watson Research Center and at GEC-Marconi Electronic Systems Corp. during the summers of 1989 and 1992, respectively. He serves as a consultant to the industry. His current research interests are signal processing, image-video compression, and pattern recognition. Dr. Akansu is an Associate Editor of *IEEE Transactions on Signal Processing*, a member of the DSP Technical Committee of the IEEE Signal Processing Society, IEEE, SPIE, and Sigma Xi. He is the coauthor of *Multiresolution Signal Decomposition: Transforms, Subbands and Wavelets*.